Short Communication

Synthesis of fct-structured FePt Nanoparticles on Graphene and their electrocatalytic activity toward Oxygen Reduction Reaction

Chia-Jen Hsu[*], Zu-Yu Pan, Yu-Ting Wu, Ching-Wei Chang and Jai-Lin Tsai[*]

Department of Materials Science and Engineering, National Chung Hsing University, Taichung, 40227, Taiwan
[*]E-mail: tsaijl@dragon.nchu.edu.tw, cxh9322@gmail.com

Face-centered tetragonal (fct) FePt nanoparticles on graphene nanosheets (fct-FePt/G) were successfully fabricated by one-pot hydrothermal synthesis and followed by heat treatment. The characterizations were examined by X-ray diffraction (XRD), vibrating-sample magnetometer (VSM), transmission electron microscopy (TEM), and electrochemical measurements. The oxygen reduction reaction (ORR) results indicate higher specific activity (~2 times) and mass activity (~12 times) of fct-FePt/G catalysts compared with commercial Pt black. The fct-FePt/G catalysts demonstrated superior electrochemical properties may due to the spin-orbit coupling between Fe (3d) and Pt (5d) which improves the Pt electrochemical activity. Also, the cooperation of graphene as the substrate would enhance the oxygen reduction reaction (ORR) due to the geometric and electronic effect between graphene and FePt nanoparticles.

1. INTRODUCTION

The Pt based alloy catalysts (Pt-M, especially 3d transition metals M= Fe, Co, and Ni) [1-3]have attracted lots of attentions in the polymer electrolyte membrane fuel cell (PEMFC) due to their superior activities toward ORR than pure Pt catalyst. The Pt combined with 3d transition metal exhibits superior oxygen adsorption on the surface of nanoparticles because of the electronic and geometric configuration, wherein FePt nanoparticles demonstrate highly electrochemical activity and longer durability. The reported synthesis methods of FePt nanoparticles with particular microstructures include template making (FePt-Fe_3O_4 nanoparticles) [4, 5], acid-etching (core-shell

FePt/Pt catalysts) [6], solution-phase self-assembly method (Graphene/FePt catalysts) [7], and hydrothermal reduction (FePt/ reduced GO catalysts) [1]. However, the magnetic and electrochemical properties of fct-FePt/G nanoparticle was rarely discussed according to the authors' best understanding.

In this study, we reported a facile one-pot synthesis of FePt nanoparticles on graphene by hydrothermal reduction method. In order to achieve ordered phase of FePt, the further thermal annealing was adopted. The ORR activity and magnetic property of synthesized fcc-FePt/G and fct-FePt/G nanoparticles will be discussed.

2. EXPERIMENTAL

The face-centered-cubic FePt/G (fcc-FePt/G) nanoparticles was synthesized via one-pot hydrothermal reaction method which mixed of 6.25 mM aqueous solution of Pt (acac)$_2$ and Fe(acac)$_3$ and 0.0075 g pristine graphene into 50 ml Teflon lined hydrothermal reactor and heated up to 200 °C for 24 hours. The fcc-FePt/G nanoparticle was rinsed several times by methanol and D.I. water, and later collected by centrifuge. The fcc-FePt/G catalysts was dried at 100°C for 24 hours. In order to achieve ordering FePt (i.e., fct-FePt/G), the further rapid thermal annealing (RTA) was performed at the temperature of 500°C for 5 minutes according to the previous study [8].

X-ray diffraction (XRD) with Cu Kα source (MAC Science, MSP-III) is scanned from 20° to 70° at the rate of 2°/min to characterize the crystalline structures. Vibrating sample magnetometer (VSM, DMS1660) was used to measure the magnetic field and moment of the materials. The high resolution transmission electronic microscopy (HR-TEM, JEOL-2010 with 200 kV accelerated voltage) equipped with selected area diffraction (SAD) was applied in nanoparticle size and crystalline structure study. The inductively coupled plasma mass spectrometry (ICP-AES, ICAP 9000) was adopted to measure the mass of Pt and Fe.

Electrochemical measurements were carry out using a Metrohm Autolab potentiostat in three electrode configurations as the rotation working electrode with glassy carbon (geometric area: 0.1963 cm^2), Pt mesh as a counter electrode, and the reference electrode via Ag/AgCl at ambient temperature. The ORR activities are carried out by rotated disc system (ALS RRDE-3A) in bubbling O$_2$-saturated 0.5 M H$_2$SO$_4$ electrolyte at 1600 rpm. The commercial 99.9 % Pt black (PtB, Alfa Aesar, CAS:7440-06-4) inks by mixing 2 mg powder in 1.5ml DI water and FePt catalysts were took 15 μl from the samples to dry on the glassy carbon electrode. Finally, 5 microliter of 5 % Nafion solution (Ion Power Inc.) was dropped onto the top of catalysts and formed a thin film at room temperature.

3. RESULTS AND DISCUSSION

Figure 1 indicates X-ray diffraction patterns of (a) commercial Pt black, (b) fcc-FePt/G and (c) fct-FePt/G samples. Pt black catalysts indicates Pt face center cubic (fcc) phase with (111), (200), and (220) reflections at 40°,46°, 68°, and 81° respectively (refer to JCPDS # 04-0802). Fcc-FePt/G sample illustrates disordered FePt fcc phase includes distinct (111), (200), and (220) reflections at 38.5°, 46°,

and 67.5° respectively (refer to JCPDS # 29-0717); fct-FePt/G catalyst shows mixed ordered/disordered ($L1_0$ fct/ fcc) phases with (001), (110), (111), (002), and (220) diffraction planes at 22.5°, 33°, 41.5°, 47°, and 68° individually (refer to JCPDS # 43-1359). Both fcc-FePt/G and fct-FePt/G display graphene (002) phase at 26° according to JCPDS # 75-1621. As the annealing temperature increase to 500°C, the ordered superlattice peaks (001) and (110) become significant. As well as the intensity of (111) peak increased indicates the ordering fct phase formed. The disordered fcc phase still exist in fct-FePt/G sample evidenced by (200) reflection.
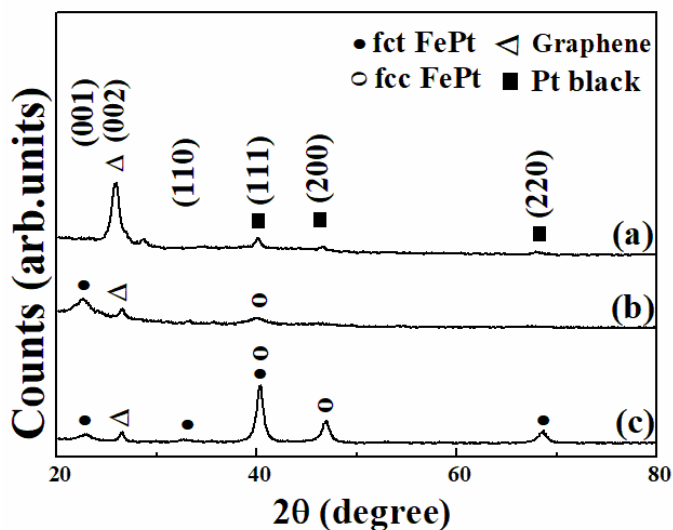

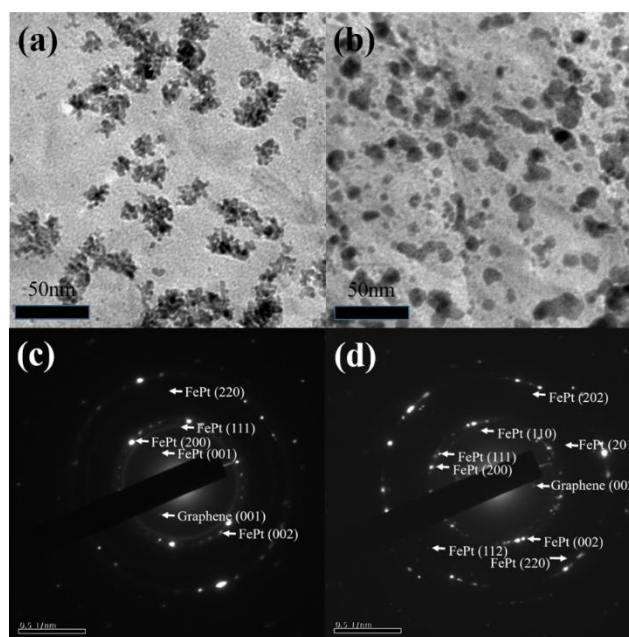**Figure 1.** XRD patterns of (a) Pt black, (b) fcc-FePt/G, (c) fct-FePt/G

Figure 2. TEM images and respective selected area diffraction (SAD) patterns of (a) fcc-FePt/G, (b) fct-FePt/G, (c) SAD of (a), (d) SAD of (b).

To further investigate insight of FePt/G nanoparticles, Figure 2 demonstrates highly dispersion of fcc-FePt/G and fct-FePt/G nanoparticles in graphene nanosheets from TEM images. The average size of fcc-FePt sample is around 4~5 nm in diameter (Figure 2a) and fct-FePt sample increases to 7~8 nm in diameter (Figure 2b) due to the thermal aggregation. Figure 2c and 2d show the structures of disordered fcc-FePt/G and ordered $L1_0$(fct)/ disordered(fcc) in fct-FePt/G sample from selected area diffraction (SAD) [9] which also confirmed from its XRD pattern.
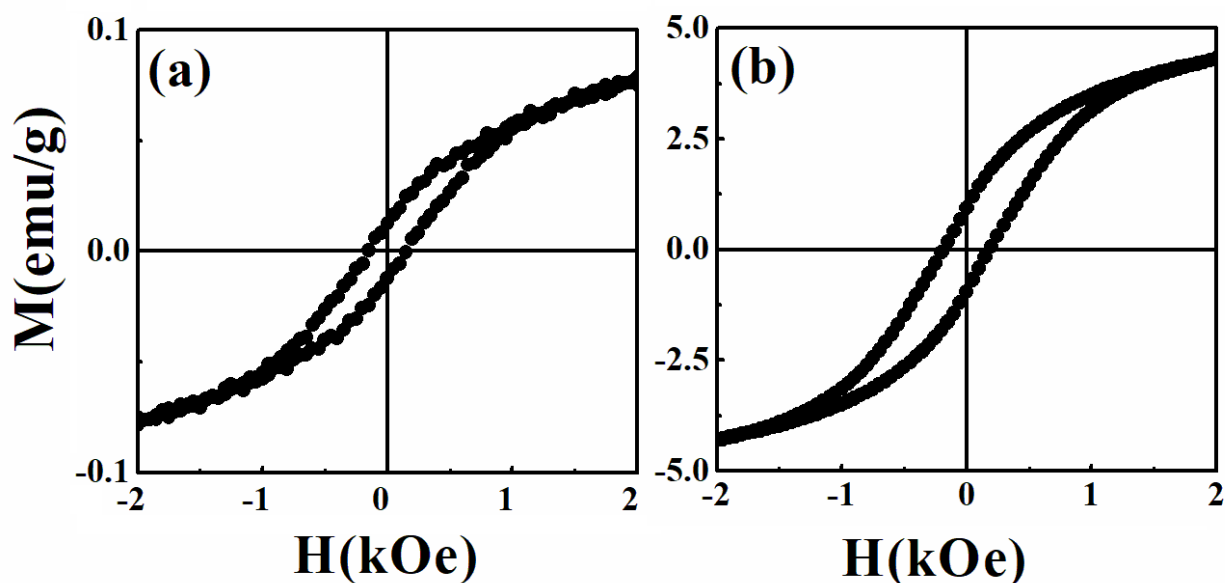

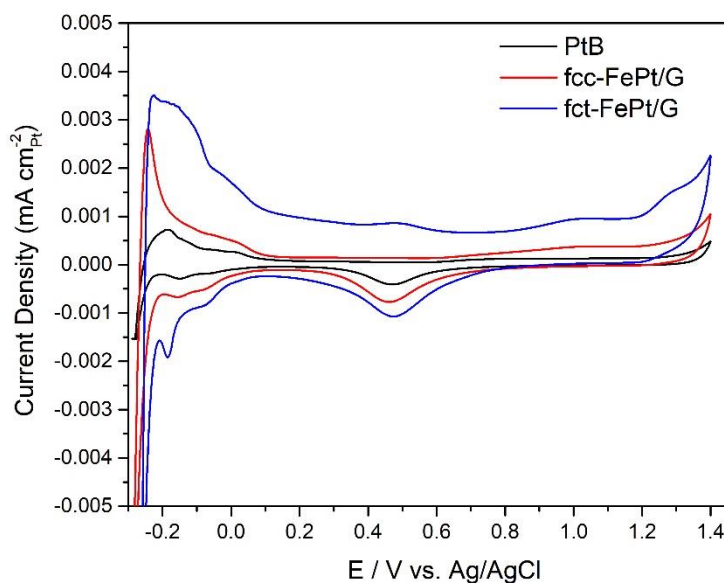**Figure 3.** Magnetic hysteresis loops of (a) fcc-FePt/G, and (b) fct-FePt/G

Figure 4. CVs of the PtB, fcc-FePt/G and fct-FePt/G samples in 0.5 M H_2SO_4 solution with 50 mV/s scan rate.

Figure 3 shows the room temperature magnetic properties of (a) fcc-FePt/G and (b) fct-FePt/G. The results show that the in-coercivity (H_c) and saturation magnetization (M_s) of the fcc-FePt/G sample at the 500 °C ordering temperature is 0.15 kOe and 0.076 emu g^{-1}; however, the H_c of fct-FePt/G sample increases to 0.19 kOe. The most significant result demonstrates that the M_s of fct-FePt/G catalyst (4.3 emu/g) boosts 56.7 times than fcc-FePt/G catalyst. The increased M_s was due to the exchange coupling of $L1_0$(fct) hard- and fcc soft- magnetic phase in fct-FePt/G sample.
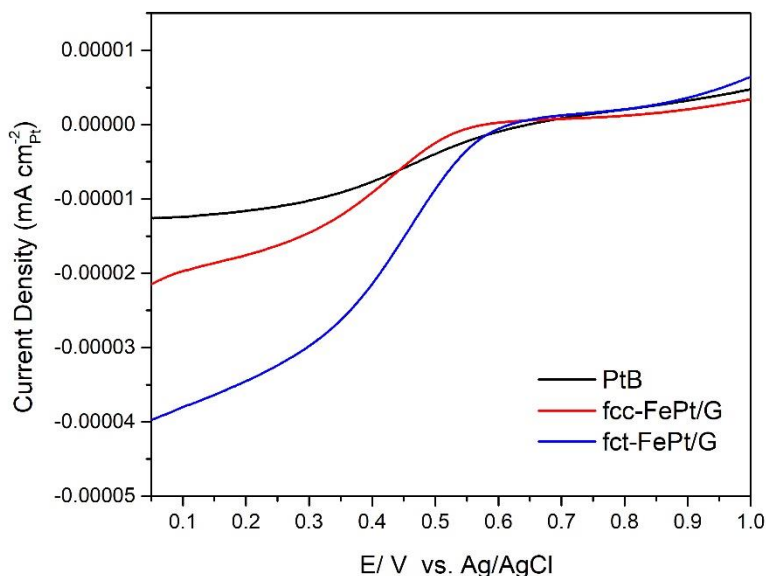

Figure 5. (a) ORR polarization curves of the PtB, fcc-FePt/G and fct-FePt/G samples in O_2-saturated 0.5 M H_2SO_4 solution with 50 mV/s scan rate at 1600 rpm rotation speed.
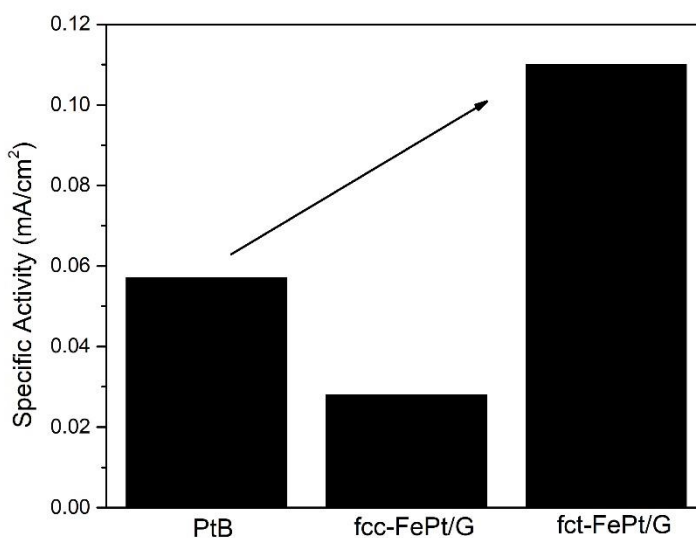

Figure 5. (b) Specific activity at 0.5 V calculation in the PtB, fcc-FePt/G and fct-FePt/G samples.
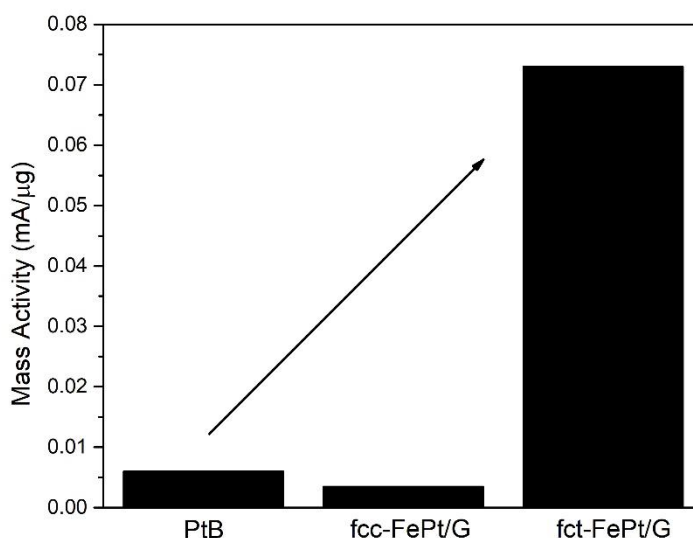
Figure 5. (c) Mass activity at 0.5 V calculation in the PtB, fcc-FePt/G and fct-FePt/G samples.

The CV curves of the synthesized catalysts measured in 0.5 M H_2SO_4 solution saturated with Ar gas are shown in Figure 4. The calculated electrochemical surface area (ECSA) from CV curves indicates that fcc-FePt/G catalysts create the highest ECSA value (12.62 m^2/g_{Pt}) due to FePt highly dispersed on graphene. However, the fct-FePt/G catalysts show the lowest ECSA value (6.44 m^2/g_{Pt}) probably due to FePt agglomeration on graphene surface after 500 °C heat treatment. Also, the PtB catalysts show intermediate ECSA value (10.22 m^2/g_{Pt}) due to small size Pt nanoparticles and porous structure. The fct-FePt/G samples exhibit well-defined hydrogen adsorption/desorption peaks and also the Pt-OH reduction peak close to 0.5 V from the CV curve. However, the PtB nanoparticles doesn't demonstrate apparently those peaks in the curve. By carefully observation, the electrical double layer (EDL) of fct-FePt/G was found larger than other samples that may attribute to the stronger electronic configuration between FePt and graphene after 500°C heat treatment. The increased EDL result of Pt/ 3D-graphene was also reported by Wang's group [10] that attributed to high surface area and conductivity of graphene.

The ORR polarization curves at 1600 rpm rotation speed in 0.5 M H_2SO_4 solution with bubbling O_2 gas for PtB, fcc-FePt/G, and fct-FePt/G are shown in Figure 5a. The onset potential of FePt/G catalysts was found the range from 0.40 V to 0.65 V (vs Ag/AgCl) which also reported by He and Crooks [11] in PdPt alloy that suggests the FePt nanoalloy catalysts with a electrochemical active Pt-skin in ORR [12]. The calculated results from ORR curves at 0.5 V are the specific activity (SA, mA cm^{-2}_{Pt}) in Figure 5b and the mass activity (MA, mA μg^{-1}_{Pt}) in Figure 5c. SA and MA were used to describe the electrochemical activity of the catalysts to replace the complex exchange current density and Tafel equation[13]. The calculation referred to the following equation[14]:

$$i_k = \frac{i_d\, i}{i_d - i} \tag{1}$$

$$MA = \frac{i_k}{m_{pt}} \tag{2}$$

$$SA = \frac{MA}{ECSA_{pt}} \tag{3}$$

where i is the experimental result from 0.5 V, i_d is the diffusion-limited current, i_k is the mass transport kinetic current, and m_{pt} is the loading of the platinum in catalysts. The kinetic currents (i_k) are used to estimate MA and SA via mass-transport correction in rotation disc test. The SA of fct-FePt/G nanoparticle (0.11 mA/cm$^2_{Pt}$) shows ~2 times of PtB (0.06 mA/cm$^2_{Pt}$) and ~ 4 times of fcc-FePt/G (0.03 mA/cm$^2_{Pt}$). The MA of fct-FePt/G samples also demostrate higher value (0.073 mA/μg$_{Pt}$) between these fcc-FePt/G samples (0.0035 mA/μg$_{Pt}$) and PtB (0.006 mA/μg$_{Pt}$). The MA of fct-FePt/G exhibits almost 12.2 times of PtB nanoparticles, implying ordered FePt will enhance the mass activity due to the geometric and electronic effect toward ORR between Fe and Pt. Stamenkovic's group also reported the effect of transition metal (Fe) to Pt, the geometric (Pt-Pt bond distance) and/or electronic structures (Pt-OH bond energy) of Pt were also changed [15] which further affect its ORR electrochemical behavior. In addition, from Chen's work [12], the FePt catalysts consisted the ratio of Fe to Pt to 42: 58 demonstrate the maximum activity for ORR in terms of the reduction overpotential and current density which was also found in this study (Fe to Pt is 43:57) due to the Pt-O interactions caused by Fe doped on the electrochemical active sites of Pt.

Table 1 summaries the reported FePt nanoparticles and their electrochemical activity in ORR. By manipulated the particle size, crystalline orientation, structure and catalyst substrates of catalysts, their results showed various higher SA and MA than control samples which provided a route to enhance the FePt electrochemical activities. Compared with their results, this study provides a facile synthesis method and exhibits better SA value and superior MA value than commercial PtB.

Table 1. ORR performance on reported FePt nanoparticles

Catalyst	Synthesis Method	MA (A g^{-1})	SA (mA cm^{-2})	Electrochemical performance	Ref.
Graphene/FePt	chemical reduction	-	1.6	SA is 5.9 times of Pt nanoparticles	[7]
8 nm Fct-FePt/C	chemical reduction	-	-	SA is 3.5 times of Pt/C	[6]
FePt-nanodendrites/C	chemical reduction	-	-	SA is 3 times of E-TEK Pt/C	[16]
FePtGO	chemical reduction	0.425	-	MA is 1.7 times of FePt	[17]
Fct-FePt Nanotubes	electrospinning	-	150	SA is 5.6 times of Pt/C	[18]

Overall, the enhanced electrochemical activities of fct-FePt/G catalyst are attributed to the bonding between FePt nanoparticle and graphene that resulted in electron transfer from graphene to FePt [19] and hence improves the adsorption of FePt nanoparticles on oxygen atoms [7].

4. CONCLUSIONS

In this study, we already provide a facile method to synthesize the fct-FePt/G nanoparticles by hydrothermal reduction and follow by annealing treatment. The fct-FePt/G catalysts show well-dispersed in the graphene matrix and maintain higher magnetic properties. Comparing with

commercial PtB and fcc-FePt/G catalysts, fct-FePt/G catalysts express superior specific activity and mass activity obtained from the ORR polarization curves. The outstanding electrochemical performance due to ordered FePt structure which affects electronic configuration between Fe and Pt. Especially, the combined graphene would also contribute electronic polarization to FePt nanoparticles. So, fct-FePt/G catalysts can be used for proton-exchange membrane fuel cells (PEMFCs).

References

1.   D. Chen, X. Zhao, S. Chen, H. Li, X. Fu, Q. Wu, S. Li, Y. Li, B.-L. Su, and R. S. Ruoff, *Carbon*, 68 (2014) 755.
2.   S. Guo, D. Li, H. Zhu, S. Zhang, N. M. Markovic, V. R. Stamenkovic, and S. Sun, *Angew. Chem. Int. Ed.*, 52 (2013) 3465.
3.   J. Snyder, K. Livi, and J. Erlebacher, *Adv. Funct. Mater.*, 23 (2013) 5494.
4.   Q. Li, L. Wu, G. Wu, D. Su, H. Lv, S. Zhang, W. Zhu, A. Casimir, H. Zhu, A. Mendoza-Garcia, and S. Sun, *Nano Lett.*, 15 (2015) 2468.
5.   J. Kim, Y. Lee, and S. Sun, *J. Am. Chem. Soc.*, 132 (2010) 4996.
6.   J. Li, Z. Xi, Y.-T. Pan, J. S. Spendelow, P. N. Duchesne, D. Su, Q. Li, C. Yu, Z. Yin, B. Shen, Y. S. Kim, P. Zhang, and S. Sun, *J. Am. Chem. Soc.*, 140 (2018) 2926.
7.   S. Guo and S. Sun, *J. Am. Chem. Soc.*, 134 (2012) 2492.
8.   C. J. Hsu, J. L. Tsai, C. W. Hsu, S. K. Chen, and W. C. Chang, *IEEE Trans. Magn.*, 42 (2006) 2900.
9.   J. L. Tsai and C. J. Hsu, *J. Phys.: Condens. Matter*, 18 (2006) 7729.
10.   T. Maiyalagan, X. Dong, P. Chen, and X. Wang, *J. Mater. Chem.*, 22 (2012) 5286.
11.   H. Ye and R. M. Crooks, *J. Am. Chem. Soc.*, 129 (2007) 3627.
12.   W. Chen, J. Kim, S. Sun, and S. Chen, *J. Phys. Chem. C*, 112 (2008) 3891.
13.   U. I. Kramm, M. Lefèvre, N. Larouche, D. Schmeisser, and J.-P. Dodelet, *J. Am. Chem. Soc.*, 136 (2014) 978.
14.   C. Hsu, C. Huang, Y. Hao, and F. Liu, *Phys. Chem. Chem. Phys.*, 14 (2012) 14696.
15.   V. Stamenković, T. J. Schmidt, P. N. Ross, and N. M. Marković, *J. Phys. Chem. B*, 106 (2002) 11970.
16.   D.-Y. Wang, H.-L. Chou, C.-C. Cheng, Y.-H. Wu, C.-M. Tsai, H.-Y. Lin, Y.-L. Wang, B.-J. Hwang, and C.-C. Chen, *Nano Energy*, 11 (2015) 631.
17.   R. Kannan, A. Silva, F. Cardoso, G. Gupta, Z. Aslam, S. Sharma, and R. Steinberger-Wilckens, *RSC Adv.*, 5 (2015) 36993.
18.   J. Lee, J. M. Yoo, Y. Ye, Y. Mun, S. Lee, O. H. Kim, H. W. Rhee, H. I. Lee, Y. E. Sung, and J. Lee, *Adv. Energy Mater.*, 5 (2015) 1402093.
19.   S. Guo, D. Wen, Y. Zhai, S. Dong, and E. Wang, *ACS nano*, 4 (2010) 3959.